Resource

Cell Reports

Piwi Proteins and piRNAs in Mammalian Oocytes and Early Embryos

Graphical Abstract

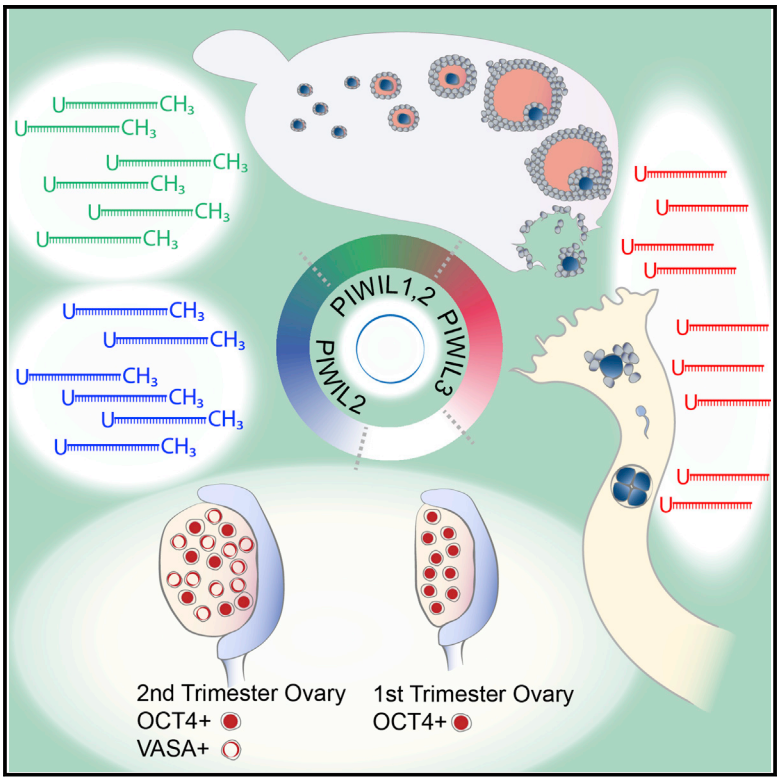

Authors

Elke F. Roovers, David Rosenkranz, ..., Bernard A.J. Roelen, René F. Ketting

Correspondence

r.ketting@imb.de

In Brief

Piwi proteins and piRNAs are essential for animal germ cells, yet their presence in mammalian oocytes has remained enigmatic. Using bovine, macaque, and human material, Roovers et al. demonstrate dynamic expression of these molecules during oogenesis. Notably, PIWIL3 is found specifically in oocytes, together with a non-methylated, adenylated piRNA population.

Highlights

- PIWIL1, PIWIL2, and PIWIL3 are dynamically expressed during mammalian oogenesis
- Human, bovine, and macaque ovaries express piRNAs that resemble piRNAs from testis
- Maturing oocytes express PIWIL3 and non-methylated, transposon-targeting piRNAs
- Predominant adenylation of piRNAs is observed in maturing oocytes and early embryos

Accession Numbers

GSE64942
PXD001741

Roovers et al., 2015, Cell Reports *10*, 2069–2082
March 31, 2015
http://dx.doi.org/10.1016/j.celrep.2015.02.062

Cell Reports
Resource

Piwi Proteins and piRNAs in Mammalian Oocytes and Early Embryos

Elke F. Roovers,[1,8] David Rosenkranz,[2,8] Mahdi Mahdipour,[3,8] Chung-Ting Han,[4] Nannan He,[5] Susana M. Chuva de Sousa Lopes,[5] Lucette A.J. van der Westerlaken,[6] Hans Zischler,[2] Falk Butter,[7] Bernard A.J. Roelen,[3,9] and René F. Ketting[1,9,*]

[1]Biology of Non-coding RNA Group, Institute of Molecular Biology (IMB), Ackermannweg 4, 55128 Mainz, Germany
[2]Johannes Gutenberg-University Mainz, Institute of Anthropology, Anselm-Franz-von-Bentzel-Weg 7, 55128 Mainz, Germany
[3]Department of Farm Animal Health, Faculty of Veterinary Medicine, Utrecht University, 3584 CM Utrecht, the Netherlands
[4]Genomics Core Facility, Institute of Molecular Biology (IMB), Ackermannweg 4, 55128 Mainz, Germany
[5]Department of Anatomy and Embryology, Leiden University Medical Center, Einthovenweg 20, 2333 ZA Leiden, the Netherlands
[6]Department of Gynaecology, Leiden University Medical Center, Albinusdreef 2, 2300RC Leiden, the Netherlands
[7]Quantitative Proteomics Group, Institute of Molecular Biology (IMB), Ackermannweg 4, 55128 Mainz, Germany
[8]Co-first author
[9]Co-senior author
*Correspondence: r.ketting@imb.de
http://dx.doi.org/10.1016/j.celrep.2015.02.062

SUMMARY

Germ cells of most animals critically depend on piRNAs and Piwi proteins. Surprisingly, piRNAs in mouse oocytes are relatively rare and dispensable. We present compelling evidence for strong Piwi and piRNA expression in oocytes of other mammals. Human fetal oocytes express PIWIL2 and transposon-enriched piRNAs. Oocytes in adult human ovary express PIWIL1 and PIWIL2, whereas those in bovine ovary only express PIWIL1. In human, macaque, and bovine ovaries, we find piRNAs that resemble testis-borne pachytene piRNAs. Isolated bovine follicular oocytes were shown to contain abundant, relatively short piRNAs that preferentially target transposable elements. Using label-free quantitative proteome analysis, we show that these maturing oocytes strongly and specifically express the PIWIL3 protein, alongside other, known piRNA-pathway components. A piRNA pool is still present in early bovine embryos, revealing a potential impact of piRNAs on mammalian embryogenesis. Our results reveal that there are highly dynamic piRNA pathways in mammalian oocytes and early embryos.

INTRODUCTION

piRNAs represent a predominantly germ-cell-specific class of small RNAs that interact with a specific class of Argonaute proteins, known as Piwi proteins (Ghildiyal and Zamore, 2009; Malone and Hannon, 2009). Both Piwi proteins and piRNAs are essential for germ cell development and function (Ketting, 2011). In their absence, germ cells can arrest during proliferation or meiosis or they can undergo apoptosis. The molecular mechanisms behind these phenotypes have not been properly described in all cases, but commonly, defects in the silencing of repetitive sequences in the genome, such as transposable elements, are important causative factors (Saito and Siomi, 2010). In line with this, piRNA populations are often enriched for transposon-derived sequences. One notable exception is the piRNA population that is expressed during spermatogenesis in mammals. These so-called pachytene piRNAs, named after the fact that they start to be expressed at the onset of pachytene stage during meiosis, are depleted of transposon-derived sequences. Therefore, this group of piRNAs could be important for additional regulatory developmental mechanisms (Gou et al., 2014; Weick and Miska, 2014), even though they can still play a role in the control of transposon activity (Di Giacomo et al., 2013).

piRNAs such as the pachytene piRNAs are derived from so-called piRNA-precursor transcripts that in turn come from large clusters that are often bi-directionally transcribed (Aravin et al., 2006; Girard et al., 2006; Lau et al., 2006). Among various mammals, the sequences of these clusters are not conserved, but their location within the genome is. The precursor transcripts are processed by a nuclease named Zucchini (Ipsaro et al., 2012; Voigt et al., 2012), after which a Piwi protein binds to the 5′ end of one of the generated fragments. This process results in piRNAs that are characterized by a strong bias for uracil at their 5′ ends, most likely because of a 5′ nucleotide preference of the Piwi protein involved (Kawaoka et al., 2011). Biogenesis is finalized by trimming of the 3′ end of the piRNA intermediate (Kawaoka et al., 2011) and 2′ O-methylation of the most 3′ base of the piRNA (Houwing et al., 2007; Vagin et al., 2006). This modification is placed by the enzyme Hen1 and serves to inhibit the addition of 3′ non-templated nucleotides, mostly uridine and adenosine, to the 3′ ends of piRNAs (Ameres et al., 2010; Horwich et al., 2007; Kamminga et al., 2010; Saito et al., 2007).

In addition to this Zucchini-driven pathway, also referred to as primary biogenesis, a secondary piRNA biogenesis mechanism exists. This has been described best in *Drosophila* oocytes,

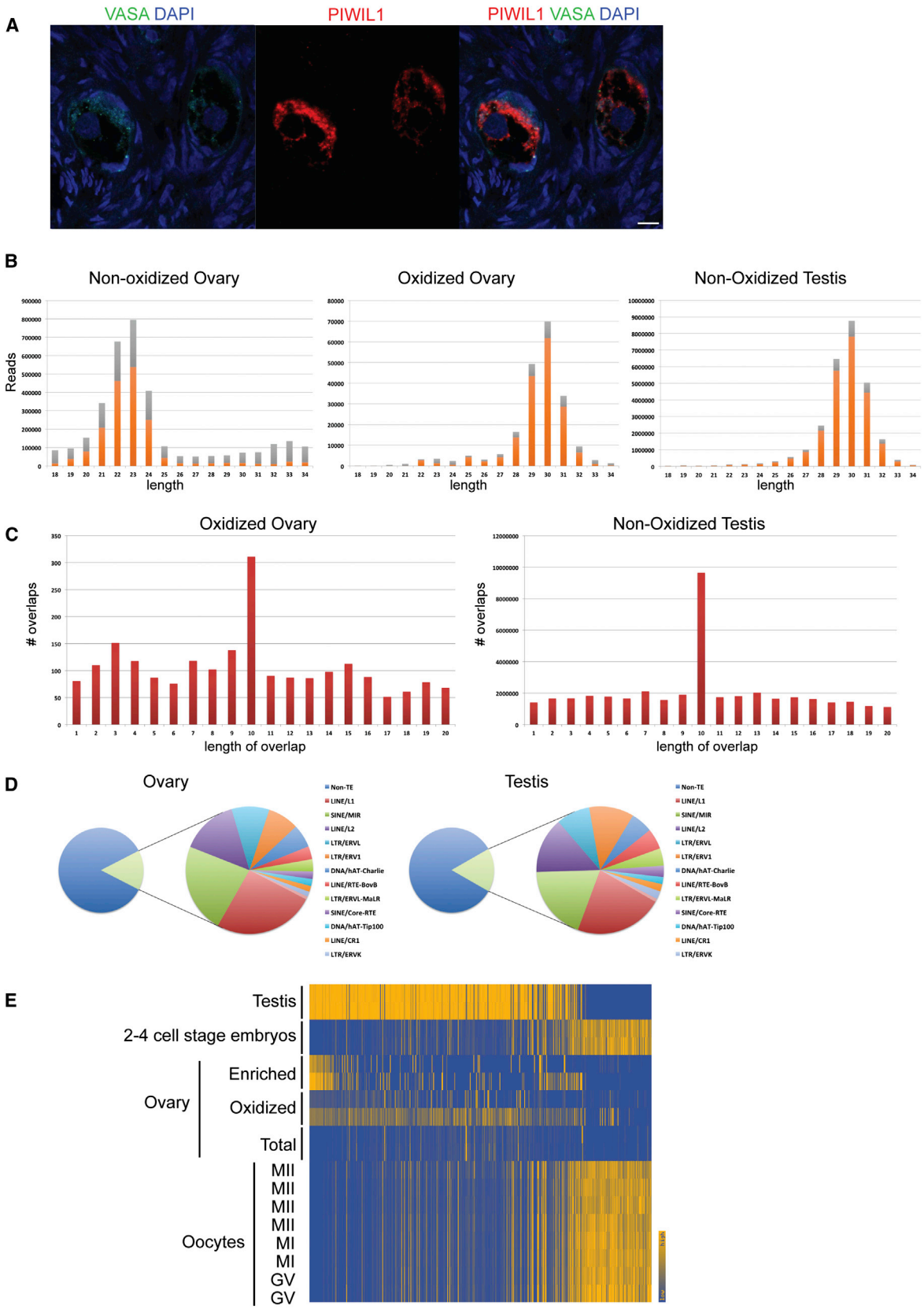

(legend on next page)

where two Piwi paralogs, Aub and Ago3, participate in this mechanism (Brennecke et al., 2007; Gunawardane et al., 2007), but operates in vertebrates as well (Aravin et al., 2007, 2008; Houwing et al., 2007, 2008). First, Aub is loaded through the primary mechanism described above. Then, when Aub cleaves a target transcript, Ago3 is loaded with the 5′ cleavage fragment generated by Aub. Reversely, when Ago3 cleaves a target RNA, an empty Aub molecule can be loaded with the generated 5′ cleavage fragment. This results in a very characteristic relationship, also known as the ping-pong signal, between the piRNAs bound by the two different Piwi paralogs: they are derived from complementary transcripts and overlap precisely ten nucleotides at their 5′ ends (Brennecke et al., 2007; Gunawardane et al., 2007). This derives from the fact that Argonaute proteins cleave their target transcripts precisely between nucleotides 10 and 11 from the 5′end of the bound small RNA. Consequently, Aub-bound piRNAs are marked by a U at position one, whereas Ago3-bound piRNAs have a characteristic adenosine enrichment at position ten.

Piwi proteins can also induce transcriptional silencing. In *Drosophila*, this is done by Piwi (Le Thomas et al., 2013; Rozhkov et al., 2013; Sienski et al., 2012), a Piwi paralog that is exclusively loaded through primary biogenesis. In mouse embryonic, male germ cells, a nuclear Piwi pathway has been shown to be driven by MIWI2 (PIWIL4) (Aravin et al., 2008; Kuramochi-Miyagawa et al., 2008). MIWI2 is specifically loaded through a secondary piRNA biogenesis mechanism, in which the Piwi-paralog MILI (PIWIL2) acts to initiate the loading of MIWI2 (Aravin et al., 2008).

In model organisms like *Drosophila* and zebrafish, Piwi proteins and piRNAs are essential during both spermatogenesis and oogenesis (Ketting, 2011). Strikingly, none of the murine Piwi proteins affect female fertility (Carmell et al., 2007; Deng and Lin, 2002; Kuramochi-Miyagawa et al., 2004). Mouse oocytes do express Piwi proteins (Aravin et al., 2008; Ding et al., 2013; Lim et al., 2013), but only relatively minor amounts of piRNAs have been detected (Tam et al., 2008; Watanabe et al., 2008). In contrast, the siRNA-generating enzyme DICER is essential for progression of mouse oocytes through meiosis (Murchison et al., 2007), paralleled by relatively high levels of siRNAs in oocytes (Tam et al., 2008; Watanabe et al., 2008). Interestingly, *Dicer* expression in mouse ovary is driven by a Muridae-specific retro-transposon insertion into the *Dicer* locus (Flemr et al., 2013). Furthermore, the mouse and rat genomes lack one of the four Piwi paralogs that are found in most other mammals, including primates and humans, PIWIL3.

We reasoned that both the lack of PIWIL3 from the mouse and rat genomes, as well as the Muridae-specific *Dicer* locus, may be indications that the small RNA status of mouse oocytes is not representative for mammals in general. We therefore profiled small RNAs from bovine, macaque, and human ovaries and from isolated, maturing bovine oocytes. We also used label-free quantitative mass spectrometry to analyze the proteome of bovine oocytes. These experiments uncovered very dynamic Piwi pathways in the female germline of these mammals, including oocyte-specific expression of PIWIL3, whereas DICER-driven pathways are only poorly represented.

RESULTS

PIWIL1 Expression in Bovine Ovary

We first tested whether Piwi proteins can be detected in adult mammalian ovarian tissue by performing immuno-fluorescence (IF) experiments on bovine (*Bos taurus*) ovarian tissue, using testis as a positive control (Figure S1A). We observed PIWIL1 expression oocytes starting at primordial stage (Figure 1A). In addition, we could also detect PIWIL1 transcripts using RT-PCR in both tissues (not shown). Whereas PIWIL1 and VASA (DDX4) displayed the typical granular structure in testis (Figure S1A), such structures were not obvious in oocytes. PIWIL2 expression was not detected in adult bovine ovary (data not shown).

Bovine Ovarian piRNAs

To follow up on the detection of PIWIL1 in bovine adult ovary, we made small RNA libraries from bovine ovary total RNA. As a comparison, we also generated small RNA libraries from testis. In both replicates of the testis, a strong peak of ~30-nucleotide piRNAs could be observed and relatively few miRNA reads (Figures 1B, S1B, and S2), consistent with previously published data on testis piRNAs in mouse, rat, and human (Aravin et al., 2006; Girard et al., 2006; Lau et al., 2006). In the ovary, however, no such population could be detected (Figures 1B and S1B). Given that the germ cell count in ovarian tissue is much lower than in testis, we reasoned that a piRNA population might be hidden by somatic small RNAs. To circumvent this, we made additional libraries of the same ovarian RNA samples following treatment with sodium periodate ($NaIO_4$). This makes most small RNA species non-accessible for cloning, except when they are protected from oxidation at their 3′ end, as piRNAs are, through 2′O-methylation (Vagin et al., 2006). Plotting only those reads from loci that are at least 5-fold enriched through this procedure, a clear piRNA-like population was detected (Figures 1B and S1B). Interestingly, the length distribution of these RNAs and their 5′ bias for uracil is virtually indistinguishable from those obtained from testis (Figure 1B). The piRNAs from testis, as well as the $NaIO_4$-enriched population from ovary, show a pronounced ping-pong signal (Figure 1C). Because the vast majority of these piRNAs are presumably bound by PIWIL1, this signature likely

Figure 1. Bovine Ovarian piRNAs

(A) Confocal image of PIWIL1 and VASA staining on bovine ovarian section. The scale bar represents 10 μm.

(B) Length profiles of the indicated libraries. Only non-annotated reads are depicted. Orange, reads starting with a U. Grey, reads not starting with a U.

(C) Overlaps of 5′ ends of reads that are mapped to opposite strands of the same locus (ping-pong signal).

(D) Diagram depicting the transposon content of bovine ovarian and testicular piRNA populations.

(E) Heatmap comparing piRNA clusters called from ovarian, testicular, and oocyte-derived (see Figure 5) piRNAs. The map is ordered according to piRNA abundance in testis clusters and reflects relative piRNA density between the various samples (highest score at each locus was set to 1 and the lowest to 0). "Enriched" refers to reads from loci that are at least 5-fold enriched following oxidation.

results from homotypic ping-pong interaction and may not play an important role in piRNA amplification. Nevertheless, it is a strong indication that these RNAs are bona fide piRNAs. The transposon-repertoires of the ovarian and testicular piRNA pools are very similar (Figures 1D, S1C, and S1D), with relatively low transposon coverage among the total small RNA pool (14% for ovary; 18% for testis). Finally, we defined piRNA clusters, using previously described software (Rosenkranz and Zischler, 2012). In testis, 564 clusters were called, representing 0.2% of the genome. More than 90% of all sequenced piRNAs can come from these loci. In ovary, 121 clusters were called (0.05% of the genome), and these can produce 84% of all piRNAs sequenced. The majority of ovarian clusters called are also represented among testis piRNA clusters (Figure 1E). Interestingly, approximately 90% of the ovarian piRNAs (defined as 5-fold enriched following oxidation) can come from testicular piRNA cluster loci. We conclude that bovine ovary expresses PIWIL1 and piRNAs that are very similar to piRNAs expressed during pachytene stage of spermatogenesis.

Ovary-Derived piRNAs from Macaque

We then turned to primates and analyzed adult macaque (*Macaca fascicularis*) ovarian and testicular tissue, using the same $NaIO_4$ treatment strategy as for bovine ovary. We now considered 2-fold enrichment, because 5-fold enrichment reduced the read numbers dramatically. Using these settings, we could clearly detect piRNA-like populations in ovarian samples of two macaque individuals (Figures 2A and S3A). Again, the length of these piRNAs is similar between testicular and ovarian samples (Figure 2A), although the ovarian piRNA population seems to be a bit broader in size. Possibly, a second, somewhat smaller piRNA population also exists next to the 30-nucleotide PIWIL1 piRNAs (see also Expression of PIWIL1 and piRNAs in Human Ovary).

With regard to transposons, the ovarian and testicular piRNA pools are similar, with the exception of ERVL and L2 (Figures 2B, S3B, and S3C). Overall, transposon coverage is again low for both ovary (14%) and testis (17%). As among bovine ovarian and testicular piRNAs, a clear ping-pong signal for macaque ovarian and testicular piRNAs is evident (Figure 2C). Finally, there is again a significant overlap between the piRNA clusters called for ovary piRNAs (264 clusters, explaining 94% of the piRNAs) and those called for testis-derived piRNAs (605 clusters, explaining 92% of the sequenced piRNAs; Figure 2D). That said, the resemblance between ovarian and testicular clusters is less convincing for macaque than for bovine piRNAs, and accordingly, only about 10% of ovarian piRNAs can come from testicular piRNA clusters. Based on these data, we conclude that also the macaque ovary expresses piRNAs in a manner that resembles pachytene piRNAs in testis, even though both tissues clearly produce unique piRNAs.

Expression of PIWIL1 and piRNAs in Human Ovary

Next, we analyzed PIWIL1 expression in human adult ovaries using IF. This revealed clear expression of PIWIL1 in oocytes that were marked by expression of VASA (Figure 3A). The staining pattern is very similar to the staining of PIWIL1 in bovine ovary. In addition to PIWIL1, and different from what we observed in bovine ovary, oocytes in human ovary also stained positive for PIWIL2 (Figure 3B). No obvious granular structures were observed for PIWIL1, PIWIL2, or VASA.

We then profiled the small RNAs of two human ovarian cortex samples from two different patients with reproductive age (Figures 3C and S4A). Following $NaIO_4$-mediated oxidation of the RNA, and considering sequences from loci that were at least 5-fold enriched, we could detect clear piRNA-like small RNAs, with characteristics that are very similar to those obtained from macaque ovary. Again, the size profile of this piRNA pool suggests the existence of two piRNA pools: one with a size of ~30 nucleotides and one that is somewhat smaller. This would be consistent with a PIWIL1- and a PIWIL2-bound piRNA pool in human ovary. In comparison, we only detected PIWIL1 in bovine ovary, and the size profile for bovine ovarian piRNAs is much sharper. Whereas we cannot prove it, our data would be consistent with a more dominant, PIWIL1-bound piRNA pool in bovine ovary compared to human and macaque ovary.

We could define only 34 human ovarian piRNA clusters that explain only 5% of the sequences that were enriched through oxidation. Possibly, the relatively low number of reads that was significantly enriched following oxidation prevents efficient cluster calling for these human samples. The oxidation-resistant RNA pool revealed a clear ping-pong signal (Figure 3D), and only 18% of these RNAs are derived from transposable elements (Figures 3E, S4B, and S4C). Overall, these results strongly suggest that adult human oocytes contain PIWIL1- and PIWIL2-bound piRNAs.

Human Fetal Oocytes Express PIWIL2

We also addressed the Piwi status of oocytes during embryonic development using IF. For this, we analyzed both first- and second-trimester ovary samples for PIWIL1 and PIWIL2. We did not detect VASA, and we did not see specific PIWIL1/2 staining in OCT4-positive cells (germ cells) in first-trimester ovaries (data not shown). However, we detect strong staining for PIWIL2 in second-trimester ovaries, especially in those germ cells that are no longer OCT4 positive but VASA positive (Figure 4A). Strikingly, both VASA and PIWIL2 localize to aggregates close to the nucleus but are both absent from the nucleus itself. This is a pattern that has been observed in mouse gonocytes as well. In fact, VASA is known to promote the ping-pong cycle (Xiol et al., 2014). In mouse gonocytes, PIWIL4 acts as the secondary Piwi protein, downstream of PIWIL2 (Aravin et al., 2008), but we could not detect convincing, germ-cell-specific staining with available PIWIL4 antibodies. Consistent with this observation, published RNA expression data (Gkountela et al., 2013) show relatively low expression of *PIWIL4* in fetal human oocytes (Figure S5D).

piRNAs from Human Fetal Ovaries

We also sequenced small RNA populations from human fetal ovaries. Two independent samples of first-trimester ovaries (8.5 and 10.5 weeks of gestation) did not yield convincing piRNA populations, whether we treated the RNA with $NaIO_4$ or not (Figure S5A). This is consistent with the fact that, during the first trimester, oocytes typically are still negative for VASA and PIWIL2 (data not shown). Strikingly, in two independent

Figure 2. Macaque Ovarian piRNAs

(A) Length profiles of the indicated libraries. Only non-annotated reads are depicted. Orange, reads starting with a U. Grey, reads not starting with a U.

(B) Diagram depicting the transposon content of macaque ovarian and testicular piRNA populations.

(C) Overlaps of 5′ ends of reads that are mapped to opposite strands of the same locus.

(D) Heatmap comparing piRNA clusters called from ovarian and testicular piRNAs. The map is ordered according to piRNA density in testicular clusters and reflects relative piRNA density between the various samples (highest score at each locus was set to 1 and the lowest to 0).

second-trimester ovaries (19 and 19.5 weeks of gestation), when VASA and PIWIL2 are strongly expressed (Figure 4A), we detect convincing piRNA-like profiles (Figures 4B and S5B), displaying a prominent ping-pong signal (Figure 4C). Roughly 50% of the oxidation-resistant RNAs can be explained by ~500 clusters. With on average 27 nucleotides, these piRNAs are significantly smaller than the 30-nucleotide piRNAs detected in the human adult ovary and their transposon-targeting capacity (30%) is higher than in the adult ovary (18%; Figures 4D, S4C, and S5C). In mouse gonocytes, the overall piRNA population peaks at 27 nucleotides as well, with a similar shoulder toward somewhat longer piRNAs (Aravin et al., 2008). For these mouse piRNAs, it was established that the overall population is in fact a merge of two piRNA populations, bound by PIWIL2 (binding

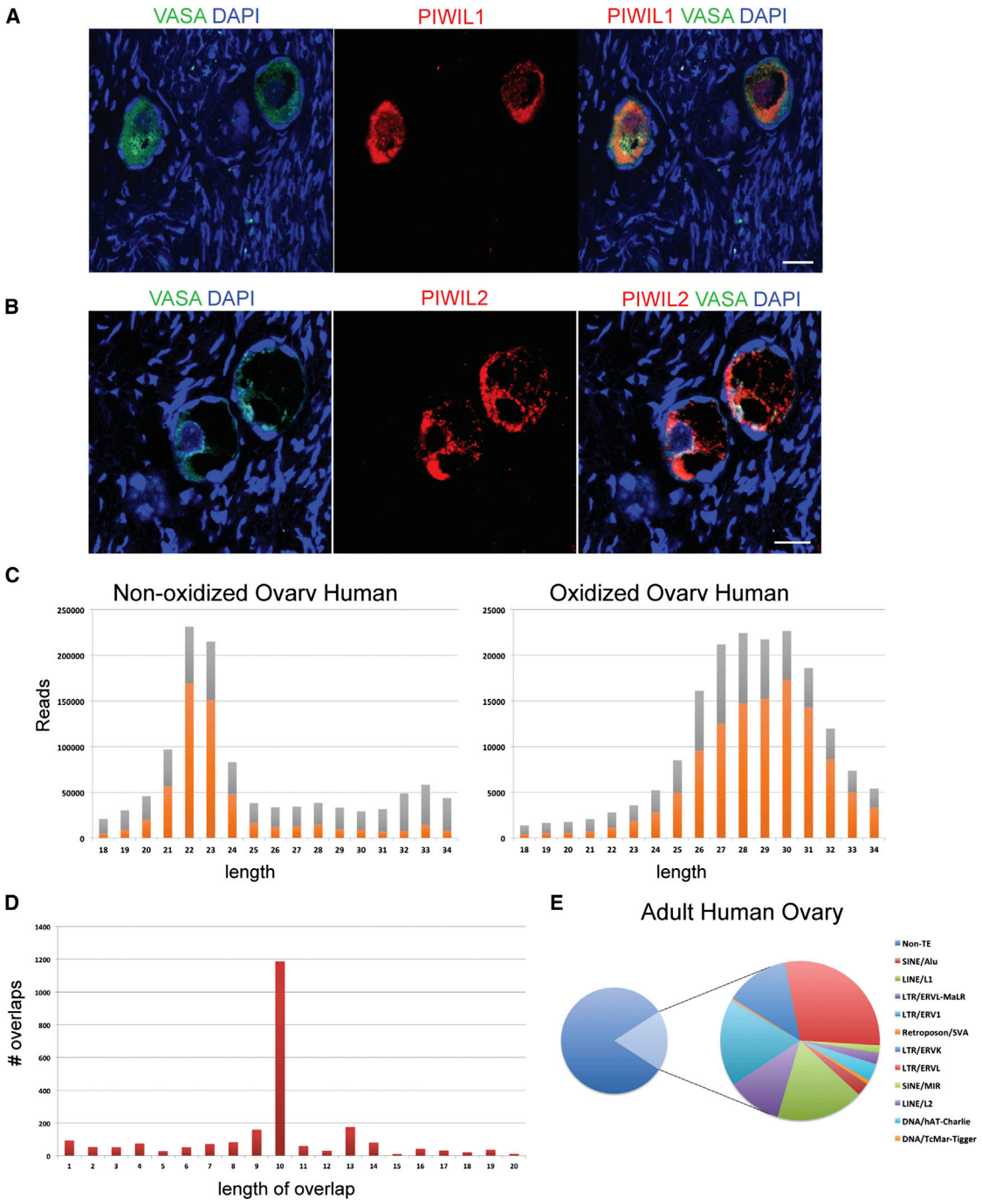

Figure 3. Human Adult Ovarian piRNAs

(A) Confocal image of PIWIL1 and VASA staining on human adult ovarian sections. The scale bar represents 15 μm.

(B) Confocal image of PIWIL2 and VASA staining on human adult ovarian sections. The scale bar represents 15 μm.

(C) Length profiles of the indicated libraries. Only non-annotated reads are depicted. Orange, reads starting with a U. Grey, reads not starting with a U.

(D) Overlaps of 5′ ends of reads that are mapped to opposite strands of the same locus.

(E) Diagram depicting the transposon content of human ovarian piRNAs.

primary piRNAs of ~26 nucleotides) and PIWIL4 (binding secondary piRNAs of ~28 nucleotides; Aravin et al., 2007, 2008). In absence of PIWIL2/4 IP data, we checked whether the sense and antisense piRNAs from the two most abundantly represented transposons (ALU and L1) displayed a significant length difference. We could, however, not detect a difference that

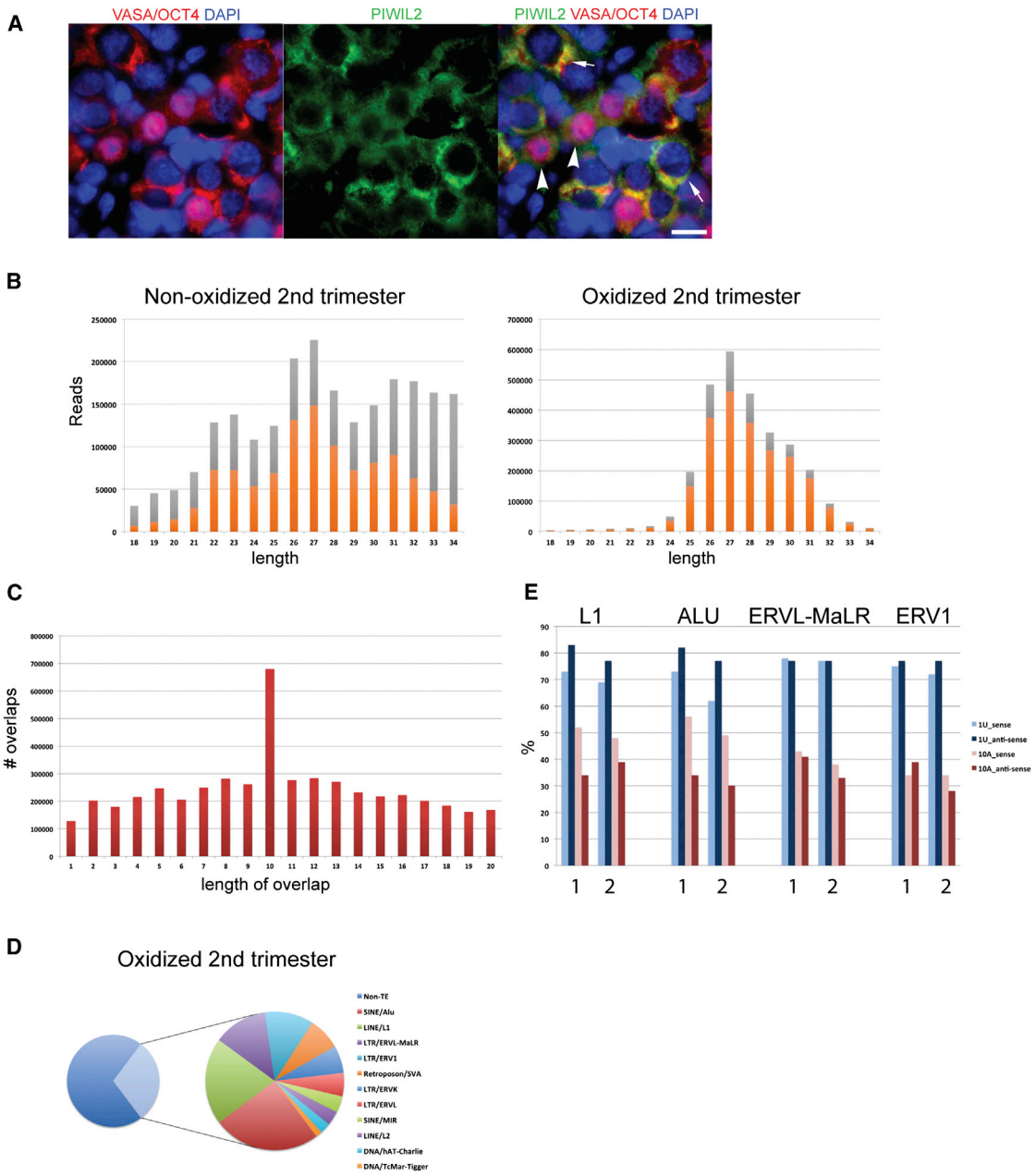

Figure 4. Human Fetal Ovarian piRNAs

(A) Wide-field image of PIWIL2 (green), VASA (red, cytoplasm), and OCT4 (red, nucleus) staining on human second-trimester ovary. Arrows indicate VASA-positive cells, and arrowheads indicate OCT4-positive cells. Note the PIWIL2 and VASA aggregates in the OCT4-negative cells. The scale bar represents 10 μm.

(B) Length profiles of the indicated libraries. Only non-annotated reads are depicted. Orange, reads starting with a U. Grey, reads not starting with a U.

(C) Overlaps of 5′ ends of reads that are mapped to opposite strands of the same locus.

(D) Diagram depicting the transposon content of second-trimester human ovarian piRNAs.

(E) 1U and 10A bias among piRNA reads derived from the indicated repetitive elements. Reads were separated according to sense or antisense polarity. Labels "1" and "2" refer to both biological replicates.

was consistent between the two fetal ovarian samples. We did detect a modest but consistent increase in 1U bias for antisense piRNAs and an increase in 10A bias for sense piRNAs for both transposon types in both samples, whereas this was absent for other abundantly represented transposons (Figure 4E). These results suggest that fetal human ovaries express piRNAs that are mostly bound by PIWIL2. A clean signature hinting at a PIWIL2-PIWIL4 interaction could not be distilled from our data.

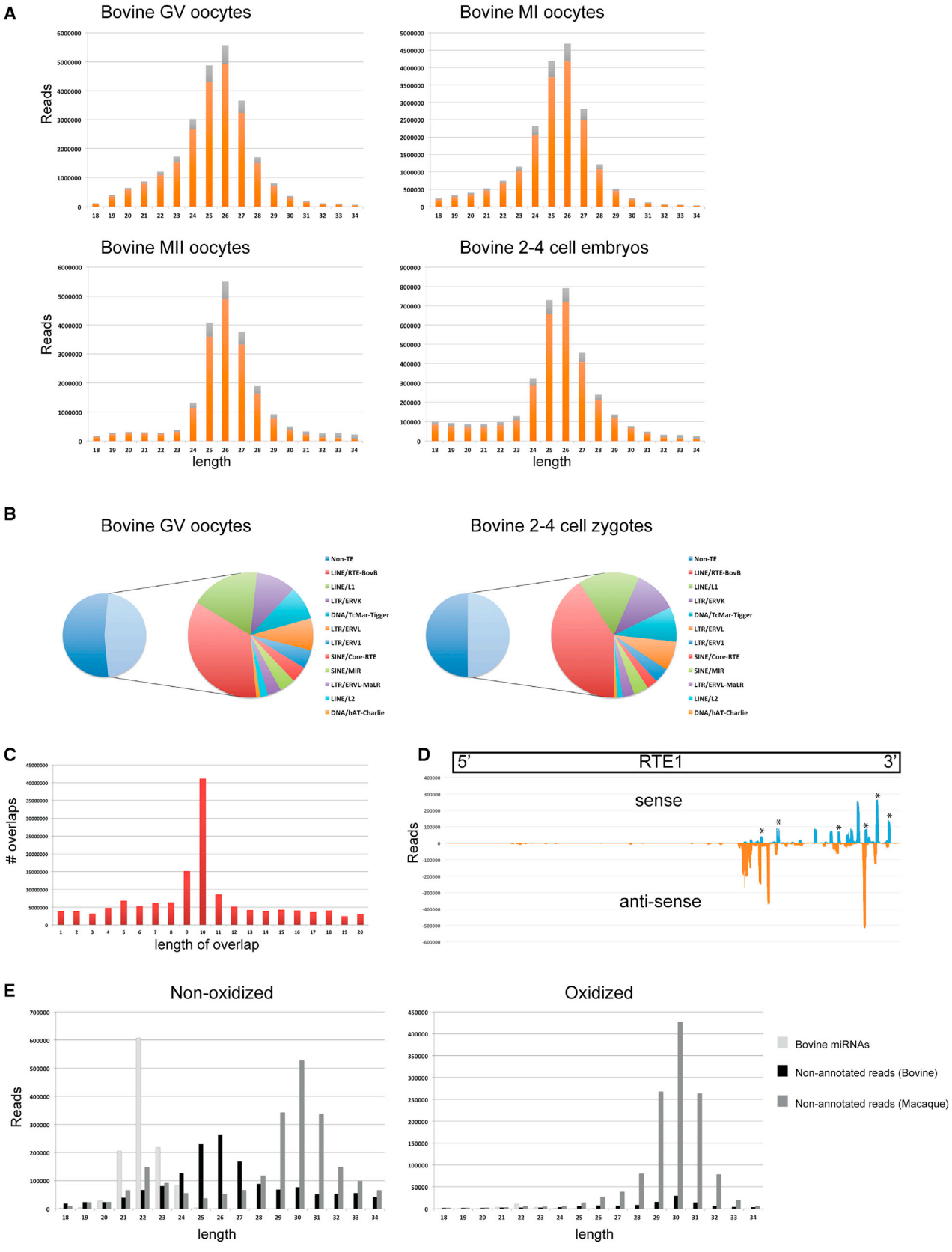

(legend on next page)

piRNAs from Isolated Bovine Oocytes from Antral Follicles

Are piRNAs still present in more mature oocytes? We tested that by generating and sequencing small RNA libraries from three independent sets of bovine germinal vesicle (GV) stage oocytes, collected from antral follicles and stripped from their accompanying cumulus cells. Less than 1% of the oocyte-derived small RNAs were miRNAs (Figure S1), and the majority of sequences were derived from a piRNA-like population (Figure 5A), ~26 nucleotides in length. These RNAs are strongly enriched for transposon sequences (more than 50%), most notably RTE1, SINE2, L1, and the endogenous retroviruses ERV1-3 (Figure 5B).

Overall, a strong ping-pong signal could be detected (Figure 5C). Both sense and antisense piRNAs from, for example, RTE1 are strongly enriched for a U at position 1 (93% and 96%, respectively) and an A at position 10 (57% and 62%, respectively), consistent with homotypic ping-pong interactions. Finally, the distribution of piRNAs along the RTE1 element shows a strong clustering of piRNAs at the 3′ end of the element, with clear signs of ping-pong interactions (Figure 5D).

We could define a set of 211 clusters that together span 0.13% of the genome and explain ~83% of the GV-stage piRNAs. These oocyte clusters are very consistent between all oocyte stages and embryos (see below) but very different from the piRNA clusters we defined based on total ovarian or testicular RNA (Figure 1E). Accordingly, less than 10% of the oocyte-derived piRNAs can come from testicular piRNA clusters.

We also matured GV stage oocytes into metaphase I (MI) and metaphase II (MII) stage oocytes and analyzed their small RNA content. Also in these stages, abundant piRNAs can be detected, and their characteristics are almost identical to those observed at the GV stage (Figures 1E and 5A). Strikingly, a very similar piRNA pool can still be detected in 2- to 4-cell-stage bovine embryos that were obtained through in vitro fertilization (IVF) (Figures 5A and 5B). No testis-derived piRNAs were obvious in these embryos, as defined by their length preference of ~30 nucleotides, indicating that paternal piRNA contribution is very limited. Based on size profiles, we could not detect a distinct population of siRNAs in any of the oocyte-derived small RNA libraries and we could not detect piRNA-like populations in the somatic cumulus cells (Figures S6A and S6B).

All oocyte and embryo libraries were made without $NaIO_4$ pretreatment, indicating that the just-described piRNA-like populations represent by far the most abundant small RNA species in these oocytes. Surprisingly, by sequencing RNA from bovine oocyte-cumulus complexes before and after $NaIO_4$ treatment, we found that the 26-nucleotide piRNAs are as sensitive to oxidation as miRNAs (Figure 5E). The oxidation efficiency in this experiment was demonstrated by the strong increase in cloning frequency of macaque testis piRNAs. These were mixed into the oocyte-cumulus RNA prior to oxidation and library preparation.

Adenylation Is Prevalent on piRNAs from Follicular Bovine Oocytes

Non-templated nucleotides at the 3′ ends of small RNAs have been described for multiple small RNA classes in multiple species (Ameres et al., 2010; Katoh et al., 2009; Li et al., 2005; van Wolfswinkel et al., 2009). Adenylation and uridylation are the most common forms of these post-transcriptional modifications. Uridylation has been coupled to target-dependent de-stabilization of small RNAs (Ameres et al., 2010), whereas adenylation has recently been shown to be involved in the clearance of maternal miRNAs (Lee et al., 2014). We therefore checked non-templated nucleotide addition in all bovine samples. In all data sets, we see that around 15% of the piRNAs is marked by such extensions of one or two nucleotides (Figure 6A). We observed a very interesting difference for non-templated nucleotides on the 26-nucleotide piRNAs from antral follicle oocytes compared to the 30-nucleotide piRNA populations. In all cases, the 30-nucleotide populations mostly displayed uridylation, whereas the 26-nucleotide piRNAs from antral oocytes displayed strong adenylation (Figure 6B). These results are consistent with the proposed role for adenylation in the clearance of maternal miRNAs in embryos. Given the abundance of piRNAs in the 2- to 4-cell-stage embryos, the maternal clearance pathway may not yet be activated in the IVF embryos we have analyzed. In accordance with this, the bovine zygotic genome is activated after the 4-cell stage (Graf et al., 2014).

PIWIL3 Is Expressed in Bovine Oocytes

To see which known Piwi-pathway- or RNAi-related proteins are expressed in oocytes, we analyzed the proteome of bovine GV- and MII-stage oocytes using label-free quantitative mass spectrometry. As comparison, we also determined the proteomes of bovine testis and of the oocyte-associated cumulus cells. In the complete data set, we identified 7,031 bovine protein groups (FDR = 0.01) and quantified 5,359 in at least half of the replicates of any sample. The individual replicates of each sample show excellent reproducibility (Figure 7A), with a correlation between 0.76 in testis and 0.94 in oocytes (Figure S7A). On the overall proteome, oocytes of both maturation stages (GV and MII) are extremely similar (Figure 7B; correlation of 0.87) but clearly distinct from testis and cumulus cells (Figures 7B and S7B). DICER and AGO2 were lowly expressed in our testis samples but escaped detection in oocytes and cumulus cells. In contrast,

Figure 5. piRNAs from Bovine Oocytes and Embryos

(A) Length profiles of the indicated libraries. Only non-annotated reads are depicted. Orange, reads starting with a U. Grey, reads not starting with a U.

(B) Diagram depicting the transposon content of bovine piRNA populations from oocytes and embryos of the indicated developmental stages.

(C) Overlaps of 5′ ends of reads that are mapped to opposite strands of the same locus.

(D) Distribution of sense and antisense piRNAs over the RTE1 element. The asterisks indicate pairs of sense and antisense piRNAs that overlap ten nucleotides at their 5′ ends.

(E) Length distribution of reads obtained from small RNA libraries made from bovine oocyte-cumulus complexes. Mixed into the RNA was macaque testis RNA. Annotated bovine miRNAs are indicated in light gray, non-annotated bovine-specific RNA fragments in black. Macaque-specific reads are in dark gray. Left panel: non-oxidized. Right panel: oxidized. Only 20% of the macaque reads are displayed in both panels in order to improve visualization of the data.

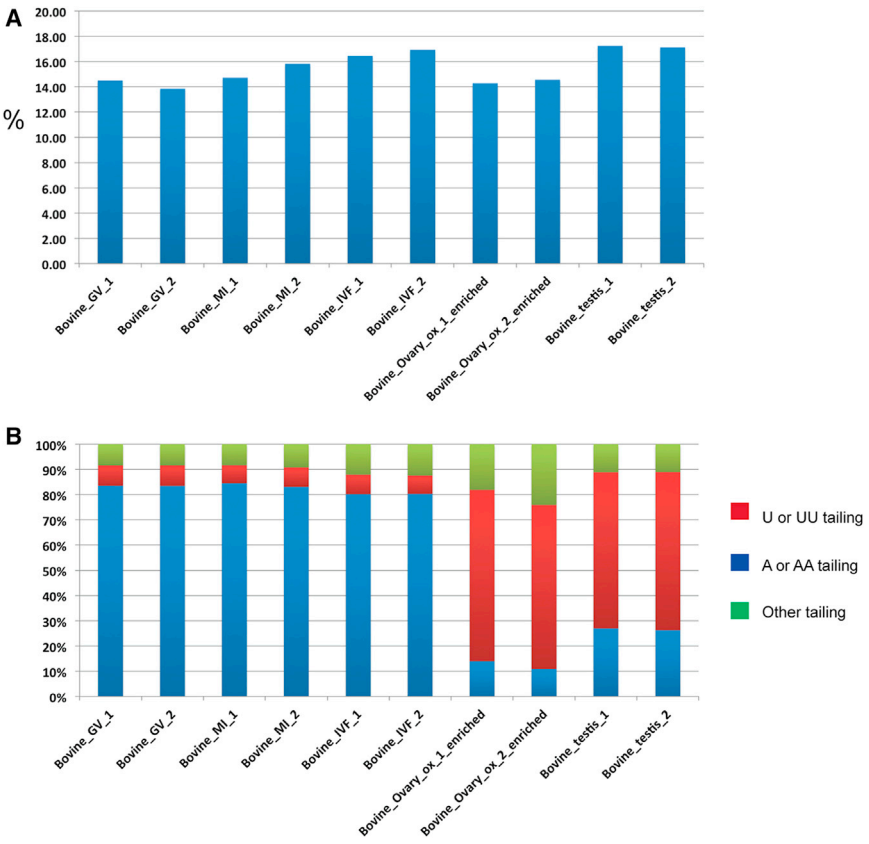

Figure 6. Non-templated Nucleotide Analysis

(A) Frequencies of non-templated bases at the 3′ end of the reads of the indicated libraries.

(B) Separation of the identified non-templated nucleotides into "A," "U," or "other" tails.

many Piwi pathway components, including PLD6, VASA, MAEL, TDRD1, and others, were expressed at significant levels in the oocytes, but not in the cumulus cells (Figure 7C). Strikingly, we detected just one of the four bovine Piwi paralogues in the oocyte samples: PIWIL3. In fact, PIWIL3 was among the most highly expressed proteins in oocytes and displayed extensive peptide coverage (Figure S7C), whereas we could not identify it in testis. In contrast, PIWIL1, and to some extent PIWIL2, both known to be expressed in testis, were easily detectable in testis (Figure 7C). Finally, in the cumulus cells, no PIWIL3 could be detected (Figures 7C and S7B). We conclude that PIWIL3 is strongly and specifically expressed in bovine oocytes from GV stage onward. We note that PIWIL3 might also be expressed during earlier stages of oogenesis.

DISCUSSION

Piwi Proteins and piRNAs in Mammalian Ovaries

In the adult ovaries of three mammalian species, we have detected populations of small RNAs that bear resemblance to the PIWIL1-bound, pachytene piRNAs found in the testis of these species. Their transposon-targeting competence is relatively limited, and hence a role outside transposon regulation seems likely. In parallel, we describe expression of PIWIL1, and in human and macaque also of PIWIL2, in oocytes.

Based on our data, we cannot determine the functions of these ovarian piRNAs, but extrapolating from work performed previously on testicular piRNAs (Aravin et al., 2007; Di Giacomo et al., 2013; Grivna et al., 2006; Hirano et al., 2014; Li et al., 2013; Robine et al., 2009; Gou et al., 2014), we may anticipate diverse roles for these piRNAs in the mammalian ovary. One of these roles could be inhibition of transposon activity. In fact, even though in mouse oocytes siRNAs are the dominating small RNA species, repressive effects of MILI on transposon-derived transcripts have been described (Lim et al., 2013; Watanabe et al., 2008). Nevertheless, no obvious effects of mouse Piwi genes on female fertility have been reported. This contrasts starkly with the strong phenotype of zebrafish *Piwi* mutant oocytes (Houwing et al., 2008). Possibly, siRNAs have taken over parts of the Piwi pathway in mouse oocytes. Indeed, *Dicer* is essential for oocyte development in mice (Murchison et al., 2007), whereas *Dicer* is non-essential in zebrafish oocytes (Giraldez et al., 2005). Extrapolating from these data, and the data we here report, we would predict that piRNAs are required for proper development of non-Muridae oocytes.

It has been shown that the transcription factor A-MYB drives pachytene piRNA cluster transcription, as well as transcription of core Piwi pathway factors, in mouse testes (Li et al., 2013). Consistent with this finding, we observe strong enrichment of A-MYB-binding sites at piRNA clusters in all our testis data sets. Whereas A-MYB sites seem to be enriched in ovarian clusters in the various species we analyzed, this enrichment does not reach significance in most cases (not shown). Interestingly, in the most deeply sequenced ovarian data set (macaque oxidized ovary; Figure 2A), A-MYB enrichment is as significant as in testis ($p < 10^{-20}$), suggesting that transcription of the ovarian clusters may also be driven by A-MYB. Possibly, the coverage of the other ovarian data sets is too limited to reach significance.

Finally, we show that the ~26-nucleotide, potentially PIWIL3-bound piRNAs in maturing oocytes (also see below) are not methylated. Hence, because we depend on oxidation to detect piRNAs in ovarian tissue, our setup would not be able to detect these ~26-nucleotide piRNAs during earlier oogenesis stages. An efficient PIWIL3-specific antibody would help to address this issue.

A Secondary piRNA Pathway in Human Fetal Ovaries?

In human fetal ovary, starting around week 9, we have uncovered a piRNA population that bears resemblances to the

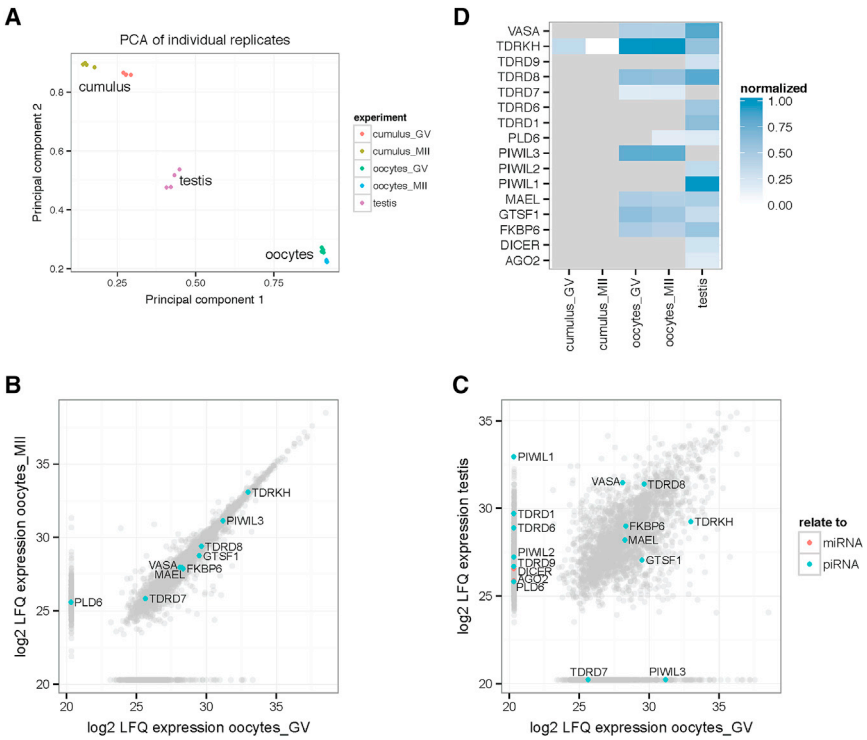

Figure 7. Quantitative Mass Spectrometry on Bovine Oocytes and Testis

(A) Principal-component analysis (PCA) calculated for the LFQ (label-free quantitation) protein expression level measured by mass spectrometry measurements show specific groups for testis, oocytes, and cumulus cells. The quadruplicate measurements cluster together according to sample type.

(B) Scatterplot comparing the LFQ expression levels of protein groups between GV- and MII-stage oocytes. Important members of the piRNA pathway are labeled. DICER and AGO1-4 involved in miRNA processing were not detectable in oocytes.

(C) Scatterplot comparing the LFQ expression levels of protein groups between GV-stage oocytes and testis. Selected piRNA (marked in blue) and miRNA (marked in red) pathway components are labeled.

(D) Heatmap showing the normalized relative expression of several piRNA- and miRNA-related proteins. PIWIL3 expression could only be detected in oocytes, whereas PIWIL1 and PIWIL2, but not PIWIL3, are expressed in testis. Grey, not detected.

MILI-MIWI2-bound piRNAs from mouse male primordial germ cells (PGCs) (Aravin et al., 2007, 2008; Kuramochi-Miyagawa et al., 2008). In human fetal ovaries, starting at the second trimester, we could detect PIWIL2, but not PIWIL1 or PIWIL4. Even though we currently lack piRNA-sequencing data from immuno-precipitates, the size profile and transposon coverage of the total piRNA population resemble the piRNA profile from mouse gonocytes closely, suggesting that PIWIL4 may be expressed in these human fetal oocytes. Everything considered, a PIWIL2-PIWIL4-driven piRNA pathway that primarily targets transposons might be active in human fetal oocytes. This should be further tested by more extensive analysis of PIWIL4 expression and, if feasible, immuno-precipitation of the Piwi proteins followed by sequencing.

PIWI Proteins and piRNAs in Mammalian Follicular Oocytes and Early Embryos

We find that oocytes of GV and MII stage and early embryos contain an abundant pool of non-2′O-methylated, ~26-nucleotide-long piRNAs that is strongly enriched for transposon-derived sequences. Given that PIWIL3 is the dominating Piwi protein in these maturing oocytes, it seems likely that this RNA pool is bound by PIWIL3. Whereas we could not detect PIWIL1 in our mass spectrometric analysis, we did detect a minor fraction of ~30-nucleotide piRNAs in one of our oocyte data sets, suggesting a relatively low expression of PIWIL1 in these later-stage oocytes. However, this particular data set was derived from a sample that also contains macaque testis RNA, and it is possible that these PIWIL1-like piRNAs are derived from non-sequenced parts of the macaque genome.

It is presently unclear whether the piRNAs in these oocytes are required for oogenesis or whether they are made to serve later. As we could not detect PIWIL3 in testis, PIWIL3 might be specialized for oocyte-specific functions or for early embryonic processes. Indeed, we can still detect these piRNAs in 2- to 4-cell-stage bovine embryos. Given the striking adenylation marks on these piRNAs, and the recent evidence that adenylation plays a role in clearing maternal miRNAs (Lee et al., 2014), it is unlikely that these piRNAs will still be present when the PGCs are specified. Hence, they most likely do not serve to prime the piRNA pathway in the PGCs, as has been described in *Drosophila* (Le Thomas et al., 2014a, b). Possibly, mammalian embryonic piRNAs act during the early embryonic genome-reprogramming steps, much like piRNAs in mouse gonocytes help to prevent transposon activity during genome reprogramming. Alternatively, these piRNAs might execute a continuous regulatory program during both oogenesis and early embryogenesis. Testing such, not mutually exclusive, hypotheses will require the establishment of a model system in which PIWIL3 is naturally expressed and in which it can be manipulated. Given the current power of genome-editing techniques, such experiments should be feasible.

PIWIL3 Loss from Muridae Oocytes?

Why have PIWIL3 and its accompanying piRNAs disappeared from mouse oocytes, and why do other mammals appear not to have a significant siRNA-mediated pathway in their oocytes? These questions can only be speculated about. The fact that the Muridae constellation, loss of PIWIL3 combined with gained expression of DICER in oocytes, is the most restricted

one, it seems reasonable to assume that a state of PIWIL3 expression combined with low levels of siRNAs represents the ancestral state that arose after the emergence of PIWIL3 in a common ancestor of eutherians. It is possible that the acquisition of DICER within the oocyte, driven by the Muridae-specific retro-transposon insertion in the *Dicer* gene (Flemr et al., 2013), had an adaptive value in maintaining PIWIL3-related functionality during and after the elimination of PIWIL3 function from ancestral populations, thus facilitating the decrease of Piwi-mediated regulation in Muridae oocytes. The fact that only PIWIL3 has been lost from the Muridae, and that PIWIL1, PIWIL2, and PIWIL4 have been conserved, is in line with our observation that only PIWIL3 specifically functions in oocytes, whereas the other Piwi paralogs are also expressed in male germ cells. Our findings reinforce the notion that piRNA pathways are extremely flexible on evolutionary timescales and that one should be very careful to extrapolate from one species to another when it comes to piRNA-related biology. In addition, we should consider an impact of Piwi/piRNAs on human reproductive biology and early embryonic development.

EXPERIMENTAL PROCEDURES

RNA Isolation, Oxidation, and Library Construction and Sequencing

Detailed information about these procedures can be found in the Supplemental Information. Library statistics and information about which library is used for which figure are provided in Table S1.

Bovine Oocytes Collection, Maturation, and Fertilization

Whole bovine ovaries and testes were collected from a local slaughterhouse and transported to the laboratory within 2 hr after slaughter at room temperature.

For oocyte collection, after washing and removal of connective tissue, the ovaries were transferred to 0.9% NaCl supplemented with 1% penicillin/streptomycin (GIBCO-BRL) and maintained at 30°C in a water bath. Cumulus oocyte complexes (COCs) were recovered by aspiration from follicles with a diameter between 2 and 8 mm. Only COCs with an intact cumulus oophorus were used for further experiments.

For the collection of MI and MII oocytes, COCs were cultured from 8 and 23 hr, respectively, in M199 medium supplemented with 12.2 mM $NaHCO_3$ at 39°C 5% CO_2 in a humidified incubator (van Tol et al., 2008). Cumulus cells were removed by vortexing for 3 min.

Embryos at the 2- to 4-cell stage were obtained by culturing COCs for 23 hr as described, after which they were co-incubated with 0.5×10^6/ml frozen-thawed sperm from a bull of proven fertility. After 20 hr, presumed zygotes were denuded by vortexing and were subsequently cultured in synthetic oviductal fluid (SOF) in a humidified incubator at 39°C 5% CO_2 and 7% O_2. At 10–14 hr of culture in SOF, 2- to 4-cell-stage embryos were snap frozen in liquid nitrogen and stored at −80°C until further use.

Immunohistochemistry

Details can be found in the Supplemental Information.

Biological Samples

Ovary (animal no. 9858, 21 years old, and 11825, 9 years old) and testis (animal no. 10787, 7 years old) tissue samples from *M. fascicularis* were provided by the German Primate Center (Deutsches Primatenzentrum [DPZ]). Human adult ovary samples used were from cancer patients that underwent unilateral oophorectomy for fertility preservation and have signed informed consent. The human fetal material used was from elective abortions and donated for research with informed consent. The research on human material was approved by the Medical Ethical Committee of the Leiden University Medical Center (CME P08.087 and CME 05/03 K/YR).

Bioinformatic Data Processing

Detailed information can be found in the Supplemental Information.

Mass Spectrometry

Samples were boiled in LDS sample buffer (Life Technologies) and separated on a 4%–12% gradient NOVEX gel (Life Technologies). Each lane was processed independently by in-gel digestions (Butter et al., 2013). Digested peptides were further separated on a 30-cm-long reverse-phase capillary (75-μm inner diameter) packed with Reprosil C18 (1.9 μm; Dr. Maisch). Peptides were eluted within a 4-hr gradient from 5%–60% acetonitrile at 200 nl/min using an Easy LC1000 HPLC system (Thermo Scientific) directly mounted to a Q Exactive Plus mass spectrometer (Thermo Scientific). The mass spectrometer was operated with a Top10 data-dependent MS/MS acquisition method per full scan. The raw files were processed with MaxQuant (Cox and Mann, 2008) standard settings, except quantitation was solely performed on unique peptides with the ENSEMBL bovine protein database (UMD3.1; 22,118 sequences). The data have been deposited to the ProteomeXchange Consortium (Vizcaíno et al., 2014) via the PRIDE partner repository with the data set identifier PXD001741. Details on data analysis can be found in the Supplemental Information.

ACCESSION NUMBERS

Sequencing data have been deposited to the NCBI GEO and are available under accession number GSE64942 and PXD001741. Proteomics data are available at the ProteomeXchange Consortium under accession number PXD001741.

SUPPLEMENTAL INFORMATION

Supplemental Information includes Supplemental Experimental Procedures, seven figures, and one table and can be found with this article online at http://dx.doi.org/10.1016/j.celrep.2015.02.062.

AUTHOR CONTRIBUTIONS

E.F.R. and M.M. executed and analyzed the experiments. D.R. performed the bioinformatic analysis. N.H., S.M.C.d.S.L., and L.A.J.v.d.W. collected human ovary material and performed IF experiments. C.-T.H. optimized small RNA-cloning procedures and made libraries. F.B. performed and analyzed the mass spectrometric analysis. H.Z. co-designed evolutionary analyses and provided primate material. B.A.J.R. provided bovine material and helped design the study. R.F.K. designed the study, interpreted the data, and wrote the manuscript. All authors contributed to and approved the final version of the manuscript.

ACKNOWLEDGMENTS

We thank Mario Dejung for help with proteomics data analysis and Leni van Tol for help with bovine oocyte collection and culture. We thank the sequencing facility at the IMSB, Johannes Gutenberg Universität Mainz for sequencing and Stefan Redl for stimulating discussions. We thank Dr. Franz-Josef Kaup and Dr. Kerstin Mätz-Rensing from the DPZ, Göttingen, for providing ovary and testis tissue samples from *M. fascicularis*. This work was supported by a VICI grant (724.011.001) from the Dutch Organization for Scientific Research (to R.F.K.), by the Rhineland-Palatinate Forschungsschwerpunkt GeneRED (to F.B. and H.Z.), by the Iranian Ministry for Science, Research and Technology (42/5/33681; to M.M.), and by the research funding program MAIFOR of the University Medical Center Mainz (to D.R.).

Received: January 9, 2015
Revised: February 12, 2015
Accepted: February 24, 2015
Published: March 26, 2015

REFERENCES

Ameres, S.L., Horwich, M.D., Hung, J.H., Xu, J., Ghildiyal, M., Weng, Z., and Zamore, P.D. (2010). Target RNA-directed trimming and tailing of small silencing RNAs. Science *328*, 1534–1539.

Aravin, A., Gaidatzis, D., Pfeffer, S., Lagos-Quintana, M., Landgraf, P., Iovino, N., Morris, P., Brownstein, M.J., Kuramochi-Miyagawa, S., Nakano, T., et al. (2006). A novel class of small RNAs bind to MILI protein in mouse testes. Nature *442*, 203–207.

Aravin, A.A., Sachidanandam, R., Girard, A., Fejes-Toth, K., and Hannon, G.J. (2007). Developmentally regulated piRNA clusters implicate MILI in transposon control. Science *316*, 744–747.

Aravin, A.A., Sachidanandam, R., Bourc'his, D., Schaefer, C., Pezic, D., Toth, K.F., Bestor, T., and Hannon, G.J. (2008). A piRNA pathway primed by individual transposons is linked to de novo DNA methylation in mice. Mol. Cell *31*, 785–799.

Brennecke, J., Aravin, A.A., Stark, A., Dus, M., Kellis, M., Sachidanandam, R., and Hannon, G.J. (2007). Discrete small RNA-generating loci as master regulators of transposon activity in Drosophila. Cell *128*, 1089–1103.

Butter, F., Bucerius, F., Michel, M., Cicova, Z., Mann, M., and Janzen, C.J. (2013). Comparative proteomics of two life cycle stages of stable isotope-labeled Trypanosoma brucei reveals novel components of the parasite's host adaptation machinery. Mol. Cell. Proteomics *12*, 172–179.

Carmell, M.A., Girard, A., van de Kant, H.J., Bourc'his, D., Bestor, T.H., de Rooij, D.G., and Hannon, G.J. (2007). MIWI2 is essential for spermatogenesis and repression of transposons in the mouse male germline. Dev. Cell *12*, 503–514.

Cox, J., and Mann, M. (2008). MaxQuant enables high peptide identification rates, individualized p.p.b.-range mass accuracies and proteome-wide protein quantification. Nat. Biotechnol. *26*, 1367–1372.

Deng, W., and Lin, H. (2002). miwi, a murine homolog of piwi, encodes a cytoplasmic protein essential for spermatogenesis. Dev. Cell *2*, 819–830.

Di Giacomo, M., Comazzetto, S., Saini, H., De Fazio, S., Carrieri, C., Morgan, M., Vasiliauskaite, L., Benes, V., Enright, A.J., and O'Carroll, D. (2013). Multiple epigenetic mechanisms and the piRNA pathway enforce LINE1 silencing during adult spermatogenesis. Mol. Cell *50*, 601–608.

Ding, X., Guan, H., and Li, H. (2013). Characterization of a piRNA binding protein Miwi in mouse oocytes. Theriogenology *79*, 610–615.e1.

Flemr, M., Malik, R., Franke, V., Nejepinska, J., Sedlacek, R., Vlahovicek, K., and Svoboda, P. (2013). A retrotransposon-driven dicer isoform directs endogenous small interfering RNA production in mouse oocytes. Cell *155*, 807–816.

Ghildiyal, M., and Zamore, P.D. (2009). Small silencing RNAs: an expanding universe. Nat. Rev. Genet. *10*, 94–108.

Giraldez, A.J., Cinalli, R.M., Glasner, M.E., Enright, A.J., Thomson, J.M., Baskerville, S., Hammond, S.M., Bartel, D.P., and Schier, A.F. (2005). MicroRNAs regulate brain morphogenesis in zebrafish. Science *308*, 833–838.

Girard, A., Sachidanandam, R., Hannon, G.J., and Carmell, M.A. (2006). A germline-specific class of small RNAs binds mammalian Piwi proteins. Nature *442*, 199–202.

Gkountela, S., Li, Z., Vincent, J.J., Zhang, K.X., Chen, A., Pellegrini, M., and Clark, A.T. (2013). The ontogeny of cKIT+ human primordial germ cells proves to be a resource for human germ line reprogramming, imprint erasure and in vitro differentiation. Nat. Cell Biol. *15*, 113–122.

Gou, L.T., Dai, P., Yang, J.H., Xue, Y., Hu, Y.P., Zhou, Y., Kang, J.Y., Wang, X., Li, H., Hua, M.M., et al. (2014). Pachytene piRNAs instruct massive mRNA elimination during late spermiogenesis. Cell Res. *24*, 680–700.

Graf, A., Krebs, S., Zakhartchenko, V., Schwalb, B., Blum, H., and Wolf, E. (2014). Fine mapping of genome activation in bovine embryos by RNA sequencing. Proc. Natl. Acad. Sci. USA *111*, 4139–4144.

Grivna, S.T., Pyhtila, B., and Lin, H. (2006). MIWI associates with translational machinery and PIWI-interacting RNAs (piRNAs) in regulating spermatogenesis. Proc. Natl. Acad. Sci. USA *103*, 13415–13420.

Gunawardane, L.S., Saito, K., Nishida, K.M., Miyoshi, K., Kawamura, Y., Nagami, T., Siomi, H., and Siomi, M.C. (2007). A slicer-mediated mechanism for repeat-associated siRNA 5′ end formation in Drosophila. Science *315*, 1587–1590.

Hirano, T., Iwasaki, Y.W., Lin, Z.Y., Imamura, M., Seki, N.M., Sasaki, E., Saito, K., Okano, H., Siomi, M.C., and Siomi, H. (2014). Small RNA profiling and characterization of piRNA clusters in the adult testes of the common marmoset, a model primate. RNA *20*, 1223–1237.

Horwich, M.D., Li, C., Matranga, C., Vagin, V., Farley, G., Wang, P., and Zamore, P.D. (2007). The Drosophila RNA methyltransferase, DmHen1, modifies germline piRNAs and single-stranded siRNAs in RISC. Curr. Biol. *17*, 1265–1272.

Houwing, S., Kamminga, L.M., Berezikov, E., Cronembold, D., Girard, A., van den Elst, H., Filippov, D.V., Blaser, H., Raz, E., Moens, C.B., et al. (2007). A role for Piwi and piRNAs in germ cell maintenance and transposon silencing in Zebrafish. Cell *129*, 69–82.

Houwing, S., Berezikov, E., and Ketting, R.F. (2008). Zili is required for germ cell differentiation and meiosis in zebrafish. EMBO J. *27*, 2702–2711.

Ipsaro, J.J., Haase, A.D., Knott, S.R., Joshua-Tor, L., and Hannon, G.J. (2012). The structural biochemistry of Zucchini implicates it as a nuclease in piRNA biogenesis. Nature *491*, 279–283.

Kamminga, L.M., Luteijn, M.J., den Broeder, M.J., Redl, S., Kaaij, L.J., Roovers, E.F., Ladurner, P., Berezikov, E., and Ketting, R.F. (2010). Hen1 is required for oocyte development and piRNA stability in zebrafish. EMBO J. *29*, 3688–3700.

Katoh, T., Sakaguchi, Y., Miyauchi, K., Suzuki, T., Kashiwabara, S., Baba, T., and Suzuki, T. (2009). Selective stabilization of mammalian microRNAs by 3′ adenylation mediated by the cytoplasmic poly(A) polymerase GLD-2. Genes Dev. *23*, 433–438.

Kawaoka, S., Izumi, N., Katsuma, S., and Tomari, Y. (2011). 3′ end formation of PIWI-interacting RNAs in vitro. Mol. Cell *43*, 1015–1022.

Ketting, R.F. (2011). The many faces of RNAi. Dev. Cell *20*, 148–161.

Kuramochi-Miyagawa, S., Kimura, T., Ijiri, T.W., Isobe, T., Asada, N., Fujita, Y., Ikawa, M., Iwai, N., Okabe, M., Deng, W., et al. (2004). Mili, a mammalian member of piwi family gene, is essential for spermatogenesis. Development *131*, 839–849.

Kuramochi-Miyagawa, S., Watanabe, T., Gotoh, K., Totoki, Y., Toyoda, A., Ikawa, M., Asada, N., Kojima, K., Yamaguchi, Y., Ijiri, T.W., et al. (2008). DNA methylation of retrotransposon genes is regulated by Piwi family members MILI and MIWI2 in murine fetal testes. Genes Dev. *22*, 908–917.

Lau, N.C., Seto, A.G., Kim, J., Kuramochi-Miyagawa, S., Nakano, T., Bartel, D.P., and Kingston, R.E. (2006). Characterization of the piRNA complex from rat testes. Science *313*, 363–367.

Le Thomas, A., Rogers, A.K., Webster, A., Marinov, G.K., Liao, S.E., Perkins, E.M., Hur, J.K., Aravin, A.A., and Tóth, K.F. (2013). Piwi induces piRNA-guided transcriptional silencing and establishment of a repressive chromatin state. Genes Dev. *27*, 390–399.

Le Thomas, A., Marinov, G.K., and Aravin, A.A. (2014a). A transgenerational process defines piRNA biogenesis in Drosophila virilis. Cell Rep. *8*, 1617–1623.

Le Thomas, A., Stuwe, E., Li, S., Du, J., Marinov, G., Rozhkov, N., Chen, Y.C., Luo, Y., Sachidanandam, R., Toth, K.F., et al. (2014b). Transgenerationally inherited piRNAs trigger piRNA biogenesis by changing the chromatin of piRNA clusters and inducing precursor processing. Genes Dev. *28*, 1667–1680.

Lee, M., Choi, Y., Kim, K., Jin, H., Lim, J., Nguyen, T.A., Yang, J., Jeong, M., Giraldez, A.J., Yang, H., et al. (2014). Adenylation of maternally inherited microRNAs by Wispy. Mol. Cell *56*, 696–707.

Li, J., Yang, Z., Yu, B., Liu, J., and Chen, X. (2005). Methylation protects miRNAs and siRNAs from a 3′-end uridylation activity in *Arabidopsis*. Curr. Biol. *15*, 1501–1507.

Li, X.Z., Roy, C.K., Dong, X., Bolcun-Filas, E., Wang, J., Han, B.W., Xu, J., Moore, M.J., Schimenti, J.C., Weng, Z., and Zamore, P.D. (2013). An ancient transcription factor initiates the burst of piRNA production during early meiosis in mouse testes. Mol. Cell *50*, 67–81.

Lim, A.K., Lorthongpanich, C., Chew, T.G., Tan, C.W., Shue, Y.T., Balu, S., Gounko, N., Kuramochi-Miyagawa, S., Matzuk, M.M., Chuma, S., et al. (2013). The nuage mediates retrotransposon silencing in mouse primordial ovarian follicles. Development *140*, 3819–3825.

Malone, C.D., and Hannon, G.J. (2009). Small RNAs as guardians of the genome. Cell *136*, 656–668.

Murchison, E.P., Stein, P., Xuan, Z., Pan, H., Zhang, M.Q., Schultz, R.M., and Hannon, G.J. (2007). Critical roles for Dicer in the female germline. Genes Dev. *21*, 682–693.

Robine, N., Lau, N.C., Balla, S., Jin, Z., Okamura, K., Kuramochi-Miyagawa, S., Blower, M.D., and Lai, E.C. (2009). A broadly conserved pathway generates 3'UTR-directed primary piRNAs. Curr. Biol. *19*, 2066–2076.

Rosenkranz, D., and Zischler, H. (2012). proTRAC—a software for probabilistic piRNA cluster detection, visualization and analysis. BMC Bioinformatics *13*, 5.

Rozhkov, N.V., Hammell, M., and Hannon, G.J. (2013). Multiple roles for Piwi in silencing Drosophila transposons. Genes Dev. *27*, 400–412.

Saito, K., and Siomi, M.C. (2010). Small RNA-mediated quiescence of transposable elements in animals. Dev. Cell *19*, 687–697.

Saito, K., Sakaguchi, Y., Suzuki, T., Suzuki, T., Siomi, H., and Siomi, M.C. (2007). Pimet, the Drosophila homolog of HEN1, mediates 2′-O-methylation of Piwi- interacting RNAs at their 3′ ends. Genes Dev. *21*, 1603–1608.

Sienski, G., Dönertas, D., and Brennecke, J. (2012). Transcriptional silencing of transposons by Piwi and maelstrom and its impact on chromatin state and gene expression. Cell *151*, 964–980.

Tam, O.H., Aravin, A.A., Stein, P., Girard, A., Murchison, E.P., Cheloufi, S., Hodges, E., Anger, M., Sachidanandam, R., Schultz, R.M., and Hannon, G.J. (2008). Pseudogene-derived small interfering RNAs regulate gene expression in mouse oocytes. Nature *453*, 534–538.

Vagin, V.V., Sigova, A., Li, C., Seitz, H., Gvozdev, V., and Zamore, P.D. (2006). A distinct small RNA pathway silences selfish genetic elements in the germline. Science *313*, 320–324.

van Tol, H.T., van Eerdenburg, F.J., Colenbrander, B., and Roelen, B.A. (2008). Enhancement of Bovine oocyte maturation by leptin is accompanied by an up-regulation in mRNA expression of leptin receptor isoforms in cumulus cells. Mol. Reprod. Dev. *75*, 578–587.

van Wolfswinkel, J.C., Claycomb, J.M., Batista, P.J., Mello, C.C., Berezikov, E., and Ketting, R.F. (2009). CDE-1 affects chromosome segregation through uridylation of CSR-1-bound siRNAs. Cell *139*, 135–148.

Vizcaíno, J.A., Deutsch, E.W., Wang, R., Csordas, A., Reisinger, F., Ríos, D., Dianes, J.A., Sun, Z., Farrah, T., Bandeira, N., et al. (2014). ProteomeXchange provides globally coordinated proteomics data submission and dissemination. Nat. Biotechnol. *32*, 223–226.

Voigt, F., Reuter, M., Kasaruho, A., Schulz, E.C., Pillai, R.S., and Barabas, O. (2012). Crystal structure of the primary piRNA biogenesis factor Zucchini reveals similarity to the bacterial PLD endonuclease Nuc. RNA *18*, 2128–2134.

Watanabe, T., Totoki, Y., Toyoda, A., Kaneda, M., Kuramochi-Miyagawa, S., Obata, Y., Chiba, H., Kohara, Y., Kono, T., Nakano, T., et al. (2008). Endogenous siRNAs from naturally formed dsRNAs regulate transcripts in mouse oocytes. Nature *453*, 539–543.

Weick, E.M., and Miska, E.A. (2014). piRNAs: from biogenesis to function. Development *141*, 3458–3471.

Xiol, J., Spinelli, P., Laussmann, M.A., Homolka, D., Yang, Z., Cora, E., Couté, Y., Conn, S., Kadlec, J., Sachidanandam, R., et al. (2014). RNA clamping by Vasa assembles a piRNA amplifier complex on transposon transcripts. Cell *157*, 1698–1711.